Gas-Phase Molecular Structure of MBBA (4-Methoxybenzylidene-4′-*n*-butylaniline), a Mesogen, by Electron Diffraction Combined with ab Initio Calculations

Nobuhiko Kuze, Hideo Fujiwara, Hiroshi Takeuchi, Toru Egawa, and Shigehiro Konaka*

Division of Chemistry, Graduate School of Science, Hokkaido University, Sapporo 060-0810, Japan

Geza Fogarasi

Department of Theoretical Chemistry, Eötvös University, Budapest, P.O. Box 32, H-1518, Hungary

Received: October 23, 1998; In Final Form: February 17, 1999

The molecular structure of a typical mesogen, 4-methoxybenzylidene-4′-*n*-butylaniline (MBBA, $CH_3O-C_6H_4-CH=N-C_6H_4-(CH_2)_3-CH_3$), has been studied by gas-phase electron diffraction (GED). The nozzle temperature was about 150 °C. Structural constraints in the GED data analysis were obtained by the ab initio MO calculation at the HF/4-21G(*) level of theory. Vibrational amplitudes and shrinkage corrections were calculated from the harmonic force constants given by a normal coordinate analysis. The phenylene ring attached to the C(=N) atom and the azomethine group (−CH=N−) are essentially on the same plane, i.e., the dihedral angle is 0(12)°. The phenylene ring bonded to the nitrogen atom is found to be out of the plane of the azomethine group and the determined value of the dihedral angle, 48(9)°, in the gas phase is larger than that in the crystalline state. This is mainly due to the steric interaction between the hydrogen atoms of the azomethine group and the phenylene ring. In the gas phase the four rotational conformers with respect to the configurations of the *n*-butyl group were assumed to exist. Their conformational abundance was fixed, as calculated from the ab initio relative energies. The principal bond distances and angles (r_g/Å and $\angle_\alpha$/deg) determined by GED are $r(N=C) = 1.290(12)$, $r(C-N) = 1.413(12)$, $r(C_{az}-C_{ring}) = 1.467(3)$, $\langle r(C_{ring}-C_{ring})\rangle = 1.400(6)$, $\angle C-N=C = 119.0(18)$, $\angle N=C-C = 121.6(13)$, $\angle NC_{ring}C_{14} = 128.5(25)$, $\angle C_{az}C_{ring}C_4 = 121.2$ (dependent), $\langle CCC_{ring}\rangle = 120.0(3)$, $\langle \angle CCC_{butyl}\rangle = 116.2(11)$, $\angle C_5C_{ring}O = 129.3$ (16), where C_{az}, C_{ring}, and C_{butyl} denote the carbon atoms of the azomethine, phenylene and butyl groups, respectively. C_{14} and C_4 are the C atoms of the rings synclinal to the C(=N) atom and cis to the H_{az} atom, and C_5 is the C atom of the ring *cis* to the C atom of the methoxy group. The values in parentheses are three times the standard deviations. The notation $\langle\ \rangle$ represents the average value. The transition temperature from the nematic to liquid phases was discussed on the basis of the determined molecular structure.

Introduction

The mesogen is a compound capable of forming liquid crystals. Although the molecular geometry is an important factor to form the liquid-crystal phase, no structural determination of the mesogen in the gas phase has been performed with the exception of *p*-azoxyanisole (PAA, $CH_3O-C_6H_4-NO=N-C_6H_4-OCH_3$)[1], which we recently investigated by gas-phase electron diffraction (GED) combined with ab initio calculations. This study showed that GED can be applied to such a large and complex system with several stable conformations. The temperature range of the nematic phase of PAA is 117−137 °C, while MBBA (4-methoxybenzylidene-4′-*n*-butylaniline, $CH_3O-C_6H_4-CH=N-C_6H_4(CH_2)_3-CH_3$) forms the nematic phase at much lower temperature, 22−47 °C. The nematic liquid crystals at room temperature are widely used and thus more important. The aim of the present work is to determine the structure of MBBA, a typical nematogen, by GED with a combined use of ab initio calculations and to investigate its characteristics. The molecule of MBBA has a fairly rigid core which consists of two phenylene rings and a linking unit (see Figure 1); that is, it is similar to that of PAA. However, MBBA has a longer and more flexible terminal substituent than PAA, i.e., *n*-butyl group. Because of the elongated molecular shape and the increased flexibility due to the *n*-butyl group, the crystal of MBBA has a lower melting point and its nematic phase has a larger temperature range than that of PAA. On the other hand, the presence of the *n*-butyl group makes it more difficult to perform structural analysis.

The crystal structures of MBBA have been investigated by X-ray diffraction.[2,3] Sereda et al.[2] performed structure analyses of MBBA on the basis of the structures of EBBA (4-ethoxybenzylidene-4′-*n*-butylaniline) and one of the fluorinated derivatives of MBBA, but no complete X-ray structure analysis of single crystals was performed because of the lack of suitable crystals. Boese et al.[3] determined the molecular structures in three different sites in the crystal at −163 °C and found that they had different conformations. In the nematic phase, the dihedral angles, $\phi_1(N_1C_2C_3C_8)$ and $\phi_2(C_2N_1C_9C_{14})$ (see Figure 1), of MBBA were determined by NMR.[4] These studies have revealed that the aromatic rings are not on the plane of the linking unit because of the internal rotation about the C_2-C_3 or C_9-N bonds. Our interests in the present study are focused on the following points: (1) how dihedrals, ϕ_1 and ϕ_2, differ in the crystal, liquid-crystal, and gas phases; (2) the effect of terminal substituents on the ϕ_1 and ϕ_2 and the geometry of the core: the electronic properties of the substituents may have an

* Corresponding author.

10.1021/jp9841384 CCC: $18.00
Published on Web 04/07/1999

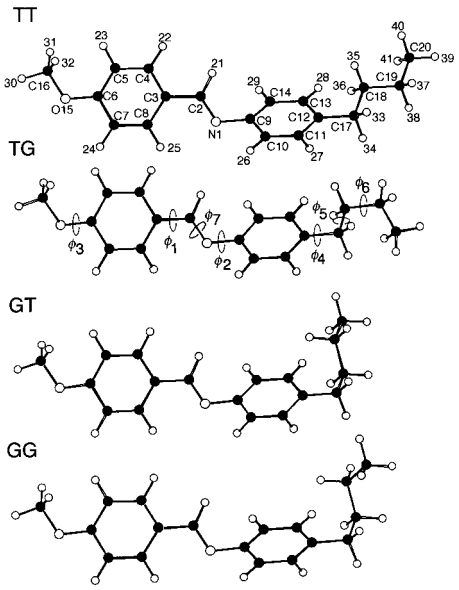

Figure 1. Molecular model of MBBA with atom numbering. ϕ_1, ϕ_2, ϕ_3, ϕ_4, ϕ_5, ϕ_6, and ϕ_7 denote dihedral angles $N_1C_2C_3C_8$, $C_2N_1C_9C_{14}$, $C_5C_6O_{15}C_{16}$, $C_{11}C_{12}C_{17}C_{18}$, $C_{12}C_{17}C_{18}C_{19}$, $C_{17}C_{18}C_{19}C_{20}$, and $C_9N_1C_2C_3$, respectively. Dihedral angle ϕ_1 is defined to be zero when the C_3-C_8 bond eclipses the N_1-C_2 bond. When looking through C_2 toward C_3, it is positive if C_8 rotates clockwise from the eclipsed position.

effect on the dihedral angles of ϕ_1 and ϕ_2;[5−8] and (3) the configuration of terminal substituents with respective to the core.

It is impossible to determine all the principal structural parameters and vibrational amplitudes of MBBA by GED alone. In such a case, the result of quantum chemical calculations is used to estimate structural constraints.[9] Therefore ab initio MO calculations of MBBA were performed and the results were used as constraints in the data analysis of GED. The molecular structure of MBBA determined by GED is compared with that obtained by ab initio calculations, the structural data by X-ray diffraction and NMR, and the gas-phase molecular structures of related compounds.

Experimental Section

The sample of MBBA with 98% purity was obtained from Tokyo Chemical Industry Co. Ltd. and used without further purification. Electron diffraction patterns were recorded on Kodak projector slide plates with an apparatus equipped with an r^3-sector[10] by using a high-temperature nozzle.[1] The temperature of nozzle tip was about 150 °C. The accelerating voltage of incident electrons was about 37 kV. Exposure times were determined by measuring the current of scattered electrons. The diffraction patterns of CS_2 were recorded at 22−24 °C in the same sequence of exposures as the sample. The photographic plates were developed for 4.5 min in Dektol developer diluted 1:1. By using a microphotometer of a double-beam autobalanced type, the optical densities of each photographic plate were measured at intervals of 36° along the circle concentric with the halo and at intervals of 0.1 mm along the diameter. Then, the raw densities measured at 50 points (10 points per circle times 5 circles) were averaged. Therefore the averaged density data were obtained at intervals of 0.5 mm along the diameter. They were converted to intensities, corrected for imperfect shape of the rotating sector and then divided by the theoretical background to obtain a leveled intensity. The leveled intensities thus obtained were averaged for three and four plates for short and long camera distances, respectively. The experimental intensities and backgrounds are available as Supporting Information (Table S1). The electron wavelength was calibrated by the known r_a(C═S) distance of CS_2 (1.5570 Å).[11] Other experimental conditions are summarized in Table 1. Elastic and inelastic atomic scattering factors were taken from refs 12 and 13. The experimental molecular scattering intensities are shown in Figure 2 along with the calculated ones in the final data analysis.

TABLE 1. Experimental Conditions

	short	long
camera distance (mm)	244.5	489.5
nozzle temperature (K)	419−430	428
electron wavelength (Å)	0.06356	0.06343
uncertainty in the scale factor (%)	0.04	0.05
background pressure during exposure (10^{-6} Torr)	1−2	1−2
beam current (μA)	2.7	2.0
exposure time (s)	60−120	37−50
number of plates used	3	4
range of s value (Å^{-1})	4.4−33.6	2.2−17.4

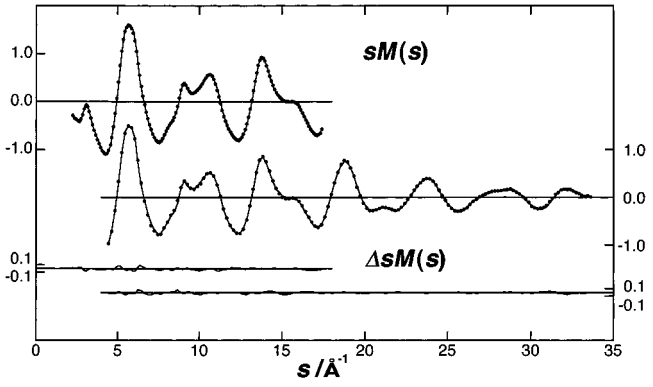

Figure 2. Experimental (dots) and theoretical (solid curves) molecular scattering intensities of MBBA; $\Delta\ sM(s) = sM(s)^{obs} - sM(s)^{calcd}$. The theoretical curves were calculated from the best fitting parameters.

The FT-Raman spectra of liquid and liquid-crystalline MBBA between 100 and 3100 cm^{-1} were observed at about 75 °C and at room temperature, respectively. They were recorded on a BOMEM DA3.16 Fourier transform spectrometer at 4 cm^{-1} resolution by using an Nd:YAG laser.

Theoretical Calculations. The searching of potential minima and full optimization of such a large system like MBBA require much CPU time even with today's computational resources available. Therefore the following steps were adopted. First, structural optimizations of two related compounds, *n*-butylbenzene ($C_6H_5-(CH_2)_3-CH_3$) and *trans*-benzylideneaniline (tBA, $C_6H_5-N{=}CH-C_6H_5$) at the HF/4-21G[14] level of theory were carried out by using the GAUSSIAN 86[15] and GAUSSIAN 92 programs[16] in order to provide the initial guess of the structure of *n*-butyl group and core of MBBA, respectively. Then, by referring to their results, four conformations of MBBA shown in Figure 1 were optimized with TX90 program system[17] employing the 4-21G(*) basis set[14,18] and empirical correction by offset forces.[18] The four conformations are denoted as TT, TG, GT, and GG, where TT represents *trans*−*trans* conformation with respect to the dihedral angles $\phi_5(C_{12}C_{17}C_{18}C_{19})$ and $\phi_6(C_{17}C_{18}C_{19}C_{20})$. Similarly, TG denotes the *trans*−*gauche* configuration. The GG′ conformer was not included in the calculation because the corresponding conformer of *n*-butylbenzene ($\phi_5 = 70°$ and $\phi_6 = -83°$) has energy higher than the GG conformer by 1.8 kcal mol^{-1}.

The 4-21G(*) basis set is the original 4-21G basis set with a set of five d functions of exponent 0.8 applied uniformly on atoms with lone pairs, i.e., nitrogen and oxygen atoms. The

option of using empirical corrections on bond lengths, to correct for systematic errors of the Hartree−Fock method, is a special feature of TX90. The corrections are made by adding offset forces along bond stretching coordinates to the ab initio potential surface during the optimization procedure. The offset forces, that had been determined in a set of small reference molecules were taken over directly from Table V of ref 18. Specifically, this means five different values according to bond types; C−C, −0.05 aJ Å^{-1}; aromatic CC, +0.10 aJ Å^{-1}; C−N and C−O, +0.02 aJ Å^{-1}; C═N, +0.26 aJ Å^{-1}; and C−H, +0.06 aJ Å^{-1}. One can estimate the effect of these forces on the bond lengths by dividing the forces by the corresponding force constants. However, the basic philosophy of the correction is different: as described in ref 18, by adding the offset forces to the ab initio potential, we modify the latter by an empirical linear term. The idea is that the neglected electron correlation energy is roughly a linear function of bond distances near equilibrium. In principle, this scheme of correction affects the geometry as a whole (due to couplings of the coordinates), but of course, the effect is significant on the bond lengths only.

Only a few optimized structural parameters showed significant conformational differences. So, those of only TT conformer are listed in Table 2 with the exception of some dihedral angles that determine conformers themselves or are substantially dependent on the conformation. See Table S2 (Supporting Information) for full description of the structural parameters of the four conformers. The inspection of Table 2 reveals some additional structural properties: (1) the phenylene ring attached to the C_2 atom is practically coplanar with the $C_3-C_2-N_1=C_9$ unit (see ϕ_1 value); (2) the other phenylene ring is twisted by about 40° (see ϕ_2 value).

Normal Coordinate Analysis. The infrared and Raman spectra of MBBA have been observed in the crystal, liquid-crystal and liquid phases by several authors.[19−24] In the present study, Raman spectra were measured in the liquid and liquid-crystal phases as stated above. Because no spectral data are available in the vapor phase, the vibrational frequencies observed in the liquid phase were used in the normal coordinate analysis. The assignments of vibrational spectra have been reported in the literature.[19,20,22,23] Some assignments were, however, corrected by referring to the assignments of the observed frequencies of related molecules such as tBA,[25−29] anisole,[30,31] benzene derivatives,[32−34] and saturated hydrocarbons.[35,36] Assignments were confirmed by normal coordinate calculations.

The force constants of MBBA have not been reported. Therefore, harmonic force constants were determined by modifying the force constants transferred from those of tBA,[25−27,29] ethers,[33,37] alkyl benzenes, [32] and saturated hydrocarbons [35] so as to reproduce the observed vibrational frequencies of MBBA. The local symmetry coordinates are defined in Table S3 and Figure S1 in the Supporting Information. Resulting force constants are summarized in Table S4 and Figure S2. The observed and calculated frequencies with potential energy distributions are listed in Table S5.

Structural Analysis. In the data analysis of GED, the following assumptions were made to reduce the number of adjustable parameters according to the results of the ab initio calculation: (1) four conformers, TT, TG, GT, and GG, coexist in the gas phase with the conformational compositions at 428 K of 43, 16, 30, and 11%, which were calculated from the energy differences obtained by the ab initio calculations; (2) the geometry of the core is common to four conformers; (3) each of the two phenylene rings and $C_3-C_2(H_{21})=N_1-C_9$ moiety takes a planar structure; (4) the differences between

TABLE 2. Optimized Geometric Parameters[a] and Relative Energies Calculated for the Four Conformers of MBBA in the ab Initio Method at the HF/4-21G(*) Level of Theory, Using Offset Forces[b]

Bond Lengths (TT Conformer)[c]					
N1−C2	1.282	C9−C14	1.402	C13−H28	1.083
N1−C9	1.421	C6−O15	1.360	C14−H29	1.081
C2−C3	1.462	O15−C16	1.426	C16−H30	1.089
C3−C4	1.393	C12−C17	1.508	C16−H31	1.094
C4−C5	1.398	C17−C18	1.536	C16−H32	1.094
C5−C6	1.397	C18−C19	1.529	C17−H33	1.095
C6−C7	1.411	C19−C20	1.528	C17−H34	1.096
C7−C8	1.380	C2−H21	1.093	C18−H35	1.096
C3−C8	1.410	C4−H22	1.084	C18−H36	1.096
C9−C10	1.403	C5−H23	1.077	C19−H37	1.097
C10−C11	1.390	C7−H24	1.079	C19−H38	1.097
C11−C12	1.403	C8−H25	1.080	C20−H39	1.094
C12−C13	1.400	C10−H26	1.081	C20−H40	1.095
C13−C14	1.395	C11−H27	1.083	C20−H41	1.095
Bond Angles (TT Conformer)[c]					
C2N1C9	117.93	C3C8H25	118.52	O15C16H30	105.69
N1C2C3	122.14	N1C9C10	117.44	O15C16H31	111.49
N1C2H21	122.23	N1C9C14	124.01	O15C16H32	111.49
C3C2H21	115.64	C10C9C14	118.51	C12C17C18	112.28
C2C3C4	120.37	C9C10C11	120.65	C12C17H33	109.75
C2C3C8	121.18	C9C10H26	118.48	C12C17H34	109.74
C4C3C8	118.46	C10C11C12	121.15	C17C18C19	112.79
C3C4C5	121.51	C10C11H27	119.46	C17C18H35	109.04
C3C4H22	119.66	C11C12C13	117.96	C17C18H36	109.07
C4C5C6	119.51	C11C12C17	120.95	C18C19C20	112.55
C4C5H23	119.28	C13C12C17	121.08	C18C19H37	109.30
C5C6C7	119.40	C12C13C14	121.30	C18C19H38	109.29
C5C6O15	125.32	C12C13H28	119.44	C19C20H39	111.30
C6C7C8	120.47	C9C14C13	120.41	C19C20H40	110.88
C6C7H24	118.04	C9C14H29	119.80	C19C20H41	110.87
C3C8C7	120.68	C6O15C16	117.42		
Dihedral Angles (TT Conformer)[c]					
C9N1C2C3 (ϕ_7)	−178.62	C14C9C10H26	178.18		
C9N1C2H21	2.20	C10C9C14C13	1.65		
C2N1C9C10	−142.43	C10C9C14H29	−176.17		
C2N1C9C14 (ϕ_2)	40.14	C9C10C11C12	1.23		
N1C2C3C4	−178.13	C9C10C11H27	−179.43		
N1C2C3C8 (ϕ_1)	1.84	H26C10C11C12	−179.14		
H21C2C3C4	1.10	C10C11C12C13	0.29		
H21C2C3C8	−178.93	C10C11C12C17	−178.45		
C2C3C4C5	179.95	H27C11C12C13	−179.06		
C2C3C4H22	−0.01	H27C11C12C17	2.21		
C4C3C8C7	0.06	C11C12C13C14	−0.82		
C4C3C8H25	−179.94	C11C12C13H28	178.34		
C3C4C5C6	−0.02	C17C12C13C14	177.92		
C3C4C5H23	−180.00	C17C12C13H28	−2.93		
C4C5C6C7	0.03	C12C13C14C9	−0.16		
C4C5C6O15	179.98	C12C13C14H29	177.66		
H23C5C6C7	−180.00	H28C13C14C9	−179.32		
C5C6C7C8	0.01	C6O15C16H30	179.99		
C5C6C7H24	179.95	C6O15C16H31	−61.34		
C5C6O15C16 (ϕ_3)	0.04	C6O15C16H32	61.33		
C6C7C8C3	−0.06	C18C19C20H39	−179.99		
C6C7C8H25	179.94	C18C19C20H40	59.86		
C14C9C10C11	−2.18	C18C19C20H41	−59.85		

Dihedral Angles (Four Conformers)				
	TT	TG	GT	GG
C11C12C17C18 (ϕ_4)	88.41	88.91	75.12	74.18
C12C17C18C19 (ϕ_5)	−179.92	177.39	65.69	63.91
C17C18C19C20 (ϕ_6)	−179.98	66.98	179.49	67.71
C11C12C17H33	−150.06	−149.98	−162.84	−162.77
C11C12C17H34	−33.10	−33.07	−46.39	−46.63
C12C17C18H35	58.07	55.66	−56.65	−58.17
C12C17C18H36	−57.90	−59.84	−172.66	−173.69
C17C18C19H37	−58.08	−171.59	−58.49	−171.20
C17C18C19H38	58.12	−55.95	57.88	−55.41
ΔE[d]	0.0	0.83	0.29	1.08

[a] Bond lengths in angstrom, angles in degree. Atom numbering is the same as shown in Figure 1. [b] Empirical offset forces are applied along the bond lengths during optimization to correct for systematic errors of the Hartree−Fock method; see the Theoretical Calculations section for the detail of the offset forces. [c] See Table S2 (Supporting Information) for the TG, GT, and GG conformers. [d] Relative energies in kcal mol^{-1}. The total energy computed for TT conformer is −821.49108215 E_h (hartree).

TABLE 3. Mean Amplitudes and Interatomic Distances of MBBA[a]

(a) Values Essentially Independent of Conformation

atom pair[b]	l_{calcd}[c]	r_a[d]	i[e]	atom pair[b]	l_{calcd}[c]	r_a[d]	i[e]	atom pair[b]	l_{calcd}[c]	r_a[d]
C−Hph[f]	0.077	1.095	1	C2···C8	0.067	2.488	2	C4···C10	0.144	5.775
C−H[f]	0.077	1.108	1	N1···C14	0.063	2.529	2	C3···C13	0.115	5.793
N1−C2	0.042	1.289	1	C4···C7	0.063	2.772	3	C3···C11	0.101	5.918
C6−O15	0.048	1.363	1	C10···C13	0.063	2.782	3	C5···C9	0.080	6.056
C7−C8	0.047	1.380	1	C11···C14	0.063	2.785	3	C7···C10	0.147	6.297
C10−C11	0.047	1.390	1	C5···C8	0.063	2.790	3	N1···O15	0.092	6.315
C3−C4	0.047	1.393	1	C3···C6	0.061	2.803	3	C8···C11	0.133	6.335
C13−C14	0.047	1.395	1	C9···C12	0.061	2.818	3	C6···C9	0.087	6.406
C5−C6	0.046	1.397	1	N1···C8	0.097	2.845	3	C3···C12	0.091	6.438
C4−C5	0.047	1.398	1	C5···C16	0.069	2.974	3	C8···C13	0.120	6.544
C12−C13	0.047	1.400	1	C2···C14	0.125	3.031	4	C2···C16	0.102	6.553
C9−C14	0.046	1.402	1	C2···C10	0.105	3.382	4	C7···C14	0.127	6.560
C11−C12	0.047	1.403	1	C8···O15	0.065	3.586	4	C4···C13	0.175	6.658
C9−C10	0.046	1.403	1	C7···C16	0.106	3.621	4	C5···C14	0.170	6.673
C6−C7	0.046	1.403	1	N1···C11	0.066	3.639	4	C5···C10	0.146	6.981
C3−C8	0.047	1.410	1	N1···C4	0.064	3.640	4	C4···C11	0.138	7.010
N1−C9	0.046	1.412	1	C3···C9	0.066	3.683	4	C8···C12	0.115	7.040
O15−C16	0.046	1.429	1	C4···O15	0.066	3.700	4	C6···C14	0.135	7.204
C2−C3	0.050	1.465	1	C2···C7	0.069	3.745	4	C6···C10	0.139	7.206
C12−C17	0.051	1.511	1	N1···C13	0.065	3.764	4	C4···C12	0.123	7.416
C19−C20	0.053	1.531	1	C2···C5	0.069	3.767	4	N1···C16	0.136	7.416
C18−C19	0.053	1.532	1	C3···O15	0.066	4.145	5	C7···C11	0.143	7.674
C17−C18	0.053	1.540	1	N1···C7	0.101	4.211	5	C9···O15	0.093	7.696
C7···O15	0.063	2.303	2	N1···C12	0.068	4.216	5	C7···C13	0.122	7.895
C2···C9	0.064	2.320	2	C8···C9	0.104	4.249	5	C5···C13	0.167	8.012
N1···C10	0.064	2.341	2	C2···C6	0.070	4.260	5	C5···C11	0.137	8.266
N1···C3	0.056	2.396	2	C4···C16	0.075	4.349	5	C7···C12	0.119	8.405
C11···C13	0.057	2.407	2	C2···C13	0.117	4.353	5	C10···O15	0.151	8.442
C4···C6	0.057	2.407	2	C3···C14	0.120	4.449	5	C14···O15	0.143	8.522
C6···C8	0.057	2.410	2	C2···C11	0.101	4.600	5	C6···C11	0.130	8.559
C4···C8	0.056	2.411	2	C3···C10	0.107	4.615	5	C6···C13	0.128	8.561
C10···C14	0.057	2.416	2	C4···C9	0.084	4.785	5	C5···C12	0.114	8.746
C6···C16	0.063	2.416	2	C8···C16	0.108	4.805	5	C9···C16	0.140	8.763
C9···C11	0.056	2.422	2	N1···C5	0.070	4.811	5	C6···C12	0.102	9.187
C9···C13	0.056	2.423	2	C8···C10	0.138	4.963	5	C14···C16	0.159	9.492
C3···C7	0.056	2.424	2	C2···C12	0.094	5.015	5	C10···C16	0.186	9.574
C10···C12	0.057	2.428	2	N1···C6	0.086	5.040	5	C11···O15	0.142	9.808
C5···C7	0.056	2.429	2	C3···C16	0.092	5.114	5	C13···O15	0.137	9.880
C12···C14	0.057	2.431	2	C8···C14	0.125	5.223	5	C12···O15	0.105	10.483
C3···C5	0.056	2.434	2	C4···C14	0.173	5.335	5	C13···C16	0.154	10.852
C5···O15	0.065	2.478	2	C2···O15	0.075	5.597		C11···C16	0.182	10.919
C2···C4	0.067	2.481	2	C7···C9	0.107	5.615		C12···C16	0.149	11.526

(b) Values Dependent on Conformation of the Butyl Group

	TT			TG			GT			GG		
atom pair[b]	l_{calcd}[c]	r_a[d]	i[e]	l_{calcd}[c]	r_a[d]	i[e]	l_{calcd}[c]	r_a[d]	i[e]	l_{calcd}[c]	r_a[d]	i[e]
N1···C17	0.074	5.719		0.074	5.718		0.074	5.724		0.074	5.722	
N1···C18	0.129	6.520		0.138	6.507		0.130	6.542		0.143	6.535	
N1···C19	0.121	7.987		0.129	7.983		0.273	6.725		0.256	6.707	
N1···C20	0.189	8.929		0.240	8.672		0.332	7.853		0.450	7.459	
C2···C17	0.096	6.498		0.104	6.502		0.101	6.503		0.104	6.500	
C2···C18	0.124	7.121		0.160	7.113		0.153	7.184		0.192	7.177	
C2···C19	0.125	8.608		0.170	8.599		0.261	7.126		0.251	7.107	
C2···C20	0.190	9.419		0.222	9.422		0.330	8.163		0.442	7.769	
C3···C17	0.094	7.930		0.098	7.932		0.096	7.933		0.100	7.929	
C3···C18	0.123	8.554		0.155	8.543		0.146	8.603		0.188	8.594	
C3···C19	0.125	10.044		0.165	10.032		0.251	8.534		0.238	8.512	
C3···C20	0.188	10.828		0.228	10.828		0.310	9.512		0.441	9.186	
C4···C17	0.122	8.872		0.124	8.878		0.131	8.875		0.147	8.871	
C4···C18	0.110	9.359		0.155	9.356		0.168	9.442		0.244	9.433	
C4···C19	0.114	10.841		0.176	10.830		0.212	9.192		0.198	9.172	
C4···C20	0.157	11.512		0.220	11.724		0.259	10.080		0.378	9.757	
C5···C17	0.114	10.215		0.116	10.216		0.124	10.212		0.139	10.209	
C5···C18	0.108	10.721		0.149	10.711		0.165	10.786		0.242	10.777	
C5···C19	0.112	12.207		0.169	12.189		0.211	10.551		0.196	10.529	
C5···C20	0.154	12.872		0.225	13.055		0.248	11.408		0.382	11.130	
C6···C17	0.105	10.684		0.108	10.684		0.109	10.683		0.112	10.680	
C6···C18	0.125	11.313		0.151	11.296		0.151	11.341		0.199	11.330	
C6···C19	0.128	12.805		0.161	12.785		0.238	11.263		0.224	11.237	
C6···C20	0.180	13.557		0.249	13.544		0.279	12.164		0.438	11.924	
C7···C17	0.124	9.904		0.126	9.906		0.128	9.913		0.128	9.908	
C7···C18	0.159	10.647		0.174	10.628		0.166	10.653		0.184	10.639	
C7···C19	0.158	12.128		0.173	12.112		0.280	10.736		0.268	10.707	
C7···C20	0.215	12.974		0.274	12.770		0.324	11.703		0.496	11.464	
C8···C17	0.120	8.540		0.123	8.540		0.126	8.548		0.127	8.542	
C8···C18	0.165	9.298		0.180	9.278		0.170	9.306		0.182	9.293	
C8···C19	0.161	10.776		0.177	10.761		0.293	9.416		0.282	9.388	
C8···C20	0.224	11.647		0.265	11.425		0.342	10.424		0.503	10.147	

TABLE 3. (continued)

	TT			TG			GT			GG		
atom pair[b]	l_{calcd}[c]	r_a[d]	i[e]	l_{calcd}[c]	r_a[d]	i[e]	l_{calcd}[c]	r_a[d]	i[e]	l_{calcd}[c]	r_a[d]	i[e]
C9···C17	0.069	4.322	5	0.069	4.322	5	0.069	4.326	5	0.069	4.326	5
C9···C18	0.126	5.162	5	0.131	5.151	5	0.125	5.194	5	0.132	5.190	5
C9···C19	0.116	6.617		0.120	6.616		0.276	5.437		0.262	5.426	
C9···C20	0.179	7.612		0.223	7.326		0.326	6.652		0.443	6.164	
C10···C17	0.071	3.807	4	0.071	3.810	4	0.071	3.817	4	0.071	3.815	4
C10···C18	0.148	4.649	5	0.155	4.639	5	0.153	4.585	5	0.154	4.574	5
C10···C19	0.149	6.052		0.148	6.067		0.301	5.109	5	0.278	5.083	5
C10···C20	0.218	7.069		0.307	6.547		0.363	6.240		0.375	6.076	
C11···C17	0.072	2.531	2	0.072	2.535	2	0.072	2.542	2	0.072	2.540	2
C11···C18	0.149	3.423	4	0.158	3.415	4	0.161	3.317	4	0.160	3.306	4
C11···C19	0.155	4.757	5	0.160	4.780	5	0.281	4.081	5	0.265	4.057	5
C11···C20	0.208	5.853		0.306	5.191	5	0.326	5.256	5	0.313	5.106	5
C12···C18	0.077	2.571	2	0.077	2.565	2	0.077	2.591	2	0.078	2.591	2
C12···C19	0.080	3.924	4	0.081	3.935	4	0.174	3.239	4	0.168	3.242	4
C12···C20	0.102	5.107	5	0.183	4.627	5	0.177	4.626	5	0.310	4.005	4
C13···C17	0.072	2.528	2	0.072	2.525	2	0.072	2.522	2	0.072	2.524	2
C13···C18	0.146	3.394	4	0.156	3.386	4	0.147	3.542	4	0.148	3.550	4
C13···C19	0.153	4.735	5	0.172	4.723	5	0.267	3.703	4	0.282	3.724	4
C13···C20	0.202	5.820		0.170	5.661		0.303	5.138	5	0.467	4.106	5
C14···C17	0.071	3.810	4	0.071	3.808	4	0.071	3.809	4	0.071	3.810	4
C14···C18	0.141	4.632	5	0.151	4.622	5	0.143	4.754	5	0.149	4.758	5
C14···C19	0.143	6.040		0.164	6.027		0.296	4.816	5	0.297	4.825	5
C14···C20	0.206	7.047		0.166	6.932		0.344	6.143		0.501	5.269	5
O15···C17	0.109	11.982		0.116	11.986		0.117	11.984		0.119	11.981	
O15···C18	0.123	12.630		0.152	12.615		0.158	12.650		0.206	12.638	
O15···C19	0.126	14.122		0.161	14.103		0.237	12.593		0.222	12.566	
O15···C20	0.173	14.877		0.265	14.831		0.271	13.477		0.443	13.269	
C16···C17	0.153	13.017		0.134	13.022		0.143	13.016		0.153	13.014	
C16···C18	0.168	13.579		0.159	13.573		0.187	13.622		0.257	13.609	
C16···C19	0.170	15.073		0.173	15.056		0.222	13.454		0.207	13.414	
C16···C20	0.209	15.753		0.262	15.850		0.245	14.281		0.400	14.061	
C17···C19	0.075	2.578	2	0.075	2.602	2	0.076	2.604	2	0.076	2.622	2
C17···C20	0.079	3.931	4	0.181	3.250	4	0.079	3.952	4	0.182	3.284	4
C18···C20	0.076	2.562	2	0.076	2.598	2	0.076	2.568	2	0.076	2.606	2

[a] Mean amplitudes and r_a distances are in angstrom unit. [b] Atom numbering is shown in Figure 1. The mean amplitudes for non-bonded atom pairs including hydrogen atom are not shown although they were included in the data analysis. C−Hph and C−H denote the bonded C−H pairs in phenylene rings and others, respectively. The values of these pairs are the averaged ones. [c] Calculated by the normal coordinate analysis at 428 K. [d] Taken from the final geometry. [e] The group of mean amplitudes (see text). The observed mean amplitudes minus calculated ones are as follows: group 1, 0.000(6) Å; group 2, −0.004(13) Å; group 3, 0.003(17) Å; group 4, −0.002(35) Å; group 5, 0.000(34) Å. Numbers in parentheses are estimated errors (3σ) for the observed values in the last significant digits. [f] Average value.

similar structural parameters are equal to those given by the ab initio calculations (see Table S6, Supporting Information); (5) the values of dihedral angles in the methoxy and *n*-butyl groups are fixed to the calculated ones; (6) the value of ∠COC is equal to the corresponding value of *p*-anisaldehyde ($CH_3O-C_6H_4-CHO$) determined by GED,[38] for the ab initio prediction of this angle seems to be too small. Thus adjustable structural parameters were taken as follows: r(C−H), $r(C-C)_{ring}$, r(C−N), r(C−C), r(N═C), ∠C═N−C, ∠N═C−C, $\angle N_1C_9C_{14}$, $\angle CCC_{ring}$, ∠CCC, ∠OCC, ϕ_1 and ϕ_2. Except for ∠COC, other bond distances and angles of the molecular skeleton are the dependent parameters of the adjustable parameters. In the preliminary analysis, the compositions of the four conformers were taken to be adjustable parameters but one of them resulted in a negative value. A similar result was obtained when the composition of GG was fixed. Therefore we concluded that it is best to fix the conformational compositions at their theoretical values (assumption 1). It is expected that the inaccuracy of the assumed abundance, which is difficult to be estimate, affects the experimentally determined core structure only slightly because the core structure is almost independent of the conformation of the *n*-butyl group.

In the theoretical calculations, only the conformers with $\phi_3(C_5C_6O_{15}C_{16}) \approx 0°$ were optimized because of the limitations of the computational resource. By the analogy of the results of the similar calculations of PAA,[1] however, it is quite possible that the conformers with $\phi_3 \approx 180°$ also exist with nearly equal energies with them for all the four forms, TT, TG, GT, and GG. At the preliminary stage, the GED analysis assuming the coexistence of the $\phi_3 \approx 0°$ and $\phi_3 = 180°$ conformers was carried out, but no other structural parameter significantly changed and no improvement of the fitting quality was obtained. Therefore only the $\phi_3 \approx 0°$ conformers were assumed in the analysis in order to reduce the computation time. Actually, those with $\phi_3 \approx 0°$ and 180° are supposed to coexist with almost the same abundance.

Vibrational amplitudes l and shrinkage corrections[39] $r_a - r_\alpha$ were calculated from the force constants obtained by the normal coordinate analysis. The small amplitude vibrational model was adopted since no reliable potential functions are available for the C−C and C−N torsions. The anharmonicity constants κ of bonded atom pairs were estimated by the conventional method,[40] while those of nonbonded atom pairs were assumed to be zero. The mean amplitudes were divided into five groups. The differences of the amplitudes in each group were fixed at the calculated values. The groups were selected according to the r_a distances, such as (i) $r_a < 2.0$ Å (the first peak of the RD curve), (ii) $r_a = 2.0-2.7$ Å (the second peak), (iii) $r_a = 2.7-3.0$ Å (the third peak), (iv) $r_a = 3.0-4.0$ Å (the fourth peak), and (v) $r_a = 4.0-5.3$ Å (the fifth and sixth peaks). Group i contains the mean amplitudes of the bonded atom pairs. The atomic pairs of group ii are related to the bond angles. Structural parameters, mean amplitudes and indices of resolution were determined by least-squares calculations on the molecular scattering intensities $sM(s)$. The mean amplitudes with the corresponding r_a distances and the grouping are listed in Table 3.

TABLE 4. Comparison of the Structural Parameters of MBBA (TT Conformer) Determined by GED with Those Geometries Calculated by ab Initio MO Methods and the Geometry Determined by X-ray Diffraction (XRD)[a]

	GED[b]		Theoretical[c]	XRD[d]
bond lengths				
$\langle C-H_{ring}\rangle$[e]	1.108(4)		1.090	
$N_1=C_2$	1.290(12)		1.282	1.284(10)
C_9-N_1	1.413(12)		1.421	1.417(8)
$\langle C-C_{ring}\rangle$[e]	1.400(6)		1.399	1.385(11)
C_2-C_3	1.467		1.462	1.479(9)
$C_{12}-C_{17}$	1.513		1.508	1.528(9)
$C_{17}-C_{18}$	1.541		1.536	1.483(12)
$C_{18}-C_{19}$	1.534	(3)	1.529	1.539(10)
$C_{19}-C_{20}$	1.533		1.528	1.524(18)
C_6-O_{15}	1.364		1.360	1.373(8)
$C_{16}-O_{15}$	1.430		1.426	1.419(12)
bond angles				
$C_2N_1C_9$	119.0(18)		117.9	119.3(7)
$N_1C_2C_3$	121.6(13)		122.1	120.5(7)
$N_1C_2H_{21}$	122.5[f]		122.2	
$N_1C_9C_{14}$	128.5(25)		124.0	125.2(9)
$C_2C_3C_4$	121.2[f]		120.4	119.6(7)
$\langle CCC_{ring}\rangle$[e]	120.0(3)		120.0	120.0(8)
$C_6O_{15}C_{16}$	122.0[g]		117.4	116.9(6)
$C_5C_6O_{15}$	129.3(16)		125.3	124.5(6)
$C_{11}C_{12}C_{17}$	121.1[f]		121.0	121.1(9)
$\langle CCC_{butyl}\rangle$[e]	116.2(11)		112.5	113.2(8)
dihedral angles				
$N_1C_2C_3C_8$ (ϕ_1)	0(12)		1.8	4
$C_2N_1C_9C_{14}$ (ϕ_2)	48(9)		40.1	24
$C_5C_6O_{15}C_{16}$ (ϕ_3)	0[g]		0.0	176
$C_{11}C_{12}C_{17}C_{18}$ (ϕ_4)	88[g]		88.4	67
$C_{12}C_{17}C_{18}C_{19}$ (ϕ_5)	180[g]		−179.9	174
$C_{17}C_{18}C_{19}C_{20}$ (ϕ_6)	180[g]		180.0	−179
$C_9N_1C_2C_3$ (ϕ_7)	180[g]		−178.6	−177
indices of resolution[h]				
k (long)	1.002(12)			
k (short)	0.933(17)			
R-factor[i]	0.038			

[a] Bond lengths in angstrom, angles in degrees. Atom numbering is shown in Figure 1. [b] The r_g distances and $\angle_\alpha$ angles. Estimated errors of 3σ in the last significant digits are given in parentheses. Errors are not listed for dependent parameters. [c] Result of the HF/4-21G(*) ab initio calculation. See the Theoretical Calculations section for the empirical correction by using offset forces. [d] Reference 3. [e] Average value. [f] Dependent parameter (see Table S6, Supporting Information). [g] Fixed parameter. [h] The index of resolution k is defined as $sM(s)^{obs} = ksM(s)^{calcd}$. [i] R-factor is defined as $R = \{\sum_i W_i(\Delta sM(s)_i)^2/\sum_i W_i(sM(s)_i^{obs})^2\}^{1/2}$, where $\Delta sM(s)_i = sM(s)_i^{obs} - sM(s)_i^{calcd}$ and W_i is a diagonal element of the weight matrix.

Results and Discussion

The final RD curve is shown in Figure 3. The good agreement between observed and calculated RD curves confirms the validity of the structural and conformational assumptions as well as the assumption of small amplitude vibrations adopted in the analysis. The observed geometry of MBBA (TT conformer) determined by GED is listed in Table 4. The estimated errors listed in this Table were calculated from three times the standard deviations of the least-squares analysis, and some of them may be somewhat optimistic. However, more precise error estimation is difficult at the present stage. The geometry of MBBA obtained by the ab initio MO calculation and that determined by X-ray diffraction are also listed in Table 4. In Table 5, the structural parameters of MBBA determined by GED are compared with those of related compounds, tBA,[41] and *N*-benzylidenemethylamine (NBMA, $C_6H_5-CH=N-CH_3$).[42] The correlation matrix in the least-squares calculation is given in Table S7, Supporting Information.

TABLE 5. Comparison of the Structures of Related Molecules[a]

	MBBA[b] MeO−C_6H_4−CH= N−C_6H_4−Bu	tBA[c] C_6H_5−CH= N−C_6H_5	NBMA[d] C_6H_5−CH= N−Me
bond lengths			
$\langle C-H\rangle$[e]	1.095(4)	1.095(10)	1.097(8)
C_2-C_3	1.465(3)	1.440(15)	1.460(11)
$\langle C-C_{ring}\rangle$[e]	1.398(6)	1.398(5)	1.401(2)
$N_1=C_2$	1.289(12)	1.284(10)	1.286(8)
C_9-N_1	1.412(12)	1.432(15)	1.463(12)
bond angles			
$C_2N_1C_9$	119.0(18)	115.0(20)	113.6(16)
$N_1C_2C_3$	121.6(13)	125.0(15)	126.5(16)
$N_1C_2H_{21}$	122.5[f]	118[g]	108.4(18)
$N_1C_9C_{14}$	128.5(25)	122.7(20)	
$C_2C_3C_4$	121.2[f]	120.0(15)	120.0[g]
$C_4C_3C_8$	118.5(3)	120.0[g]	
dihedral angles			
$\phi_1(N_1C_2C_3C_8)$	0(12)	0(15)	0[g]
$\phi_2(C_2N_1C_9C_{14})$	48(9)	52(5)	

[a] Bond lengths in angstrom, angles in degrees. Atom numbering is shown in Figure 1. [b] This work (r_a and $\angle_\alpha$). Estimated errors in parentheses are 3σ. [c] Reference 41 (r_a and $\angle_\alpha$). Limits of error were estimated from the shape of the squared-error-sum functions near the minimum values. [d] Reference 42 (r_a and $\angle_\alpha$). Values in parentheses are the estimated limits of error (3σ). [e] Average value for the phenylene or phenyl group. [f] Dependent parameter (see Table S6, Supporting Information). [g] Fixed parameter.

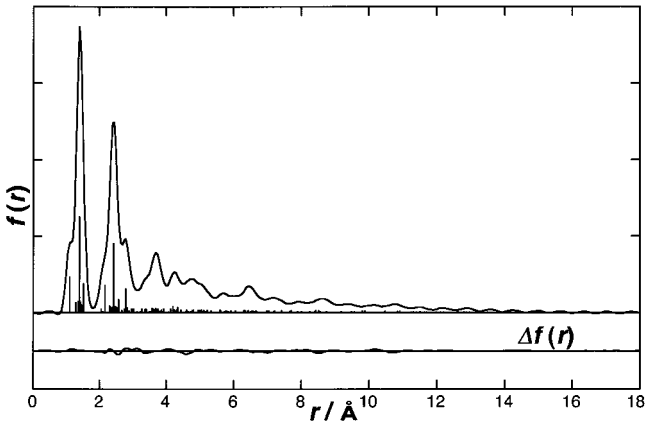

Figure 3. Experimental radial distribution curve of MBBA; $\Delta f(r) = f(r)^{obs} - f(r)^{calcd}$. Distance distributions are indicated by vertical bars.

1. Comparison between Experimental and Theoretical Structures. The values of ϕ_1 and ϕ_2 determined by GED are 0(12)° and 48(9)°, respectively, which are close to the ab initio 4-21G(*) values, 2° and 40°, respectively. Therefore it can be said that the ab initio calculation at the HF/4-21G(*) level well predicts the conformation of the core of MBBA. The determined value of $\angle N_1C_9C_{14}$, 128.5(25)°, is larger than its ab initio prediction, 124.0°. The values for the parameters of the linking unit of MBBA (r(N=C), $r(C_2-C_3)$, $\angle C_2N_1C_9$, and $\angle N_1C_2C_3$) agree with the experimental ones within the error limits. On the other hand, the calculation underestimates the bond angles of the side chains, COC and CCC_{butyl}. As for the COC angle, for which the corresponding value for *p*-anisaldehyde, 122.0°, was used, we also tried the data analysis by using the ab initio value of 117.4°, which provided poorer agreement between observed and calculated $sM(s)$. The HF/4-21G(*) calculation underestimates the $\angle$COC by about 5° also in the case of PAA.[1]

2. Comparison between the Structures of MBBA and Those of Related Compounds. The experimental values of the C−H and $C-C_{ring}$ distances in the phenylene ring and the N=C distance of MBBA are in agreement with the corresponding

distances of tBA and NBMA. The r_a (C_2-C_3) of MBBA, 1.465(3) Å, is slightly longer than that of tBA, 1.440(15) Å, and is comparable with that of NBMA, 1.460(11) Å. In these molecules, the central azomethine group and the phenyl ring bonded to the carbon atom are almost coplanar. Therefore, the C_2-C_3 bonds in these compounds were shorter than the $C_{12}-C_{17}$ bond of MBBA because of the π-character of this bond increased by coplanarity.[41] Both of the C_9-N bond lengths of MBBA and tBA are shorter than that of NBMA. This is consistent with the tendency that $r(C-N)_{aliphatic}$ is larger than $r(C-N)_{aromatic}$ as mentioned by Vilkov and Sadova.[43]

The C═N−C and N═C−C angles of MBBA are different from those of tBA. The $N_1C_9C_{14}$ angle of MBBA is larger than that of tBA. These differences in the bond angles as well as the differences in the C_2-C_3 and N_1-C_9 distances are considered to be due to the terminal substituents in MBBA.

The $r_g(C_6-O)$ and $r_g(C_{16}-O)$ distances of MBBA, 1.364(6) and 1.430(6) Å, agree well with the corresponding parameters of anisole,[44] 1.362(15) and 1.425(15) Å, *p*-anisaldehyde,[38] 1.358(12) and 1.420(10) Å, and PAA[1], 1.350(1) and 1.421(1) Å.

The core of MBBA is not planar according to the data analysis of GED. Its ϕ_2 value, 48(9)°, is in agreement with that of tBA, 52(5)°. The ϕ_1 values of MBBA and tBA are found to be zero as in the case of NBMA.

In the case of tBA molecule, conformational stability with respect to ϕ_2 is mainly determined by the steric repulsion between the orthohydrogen atoms corresponding to H_{21} and H_{29} of MBBA.[41] The $H_{21}\cdots H_{29}$ distance of MBBA, 2.56 Å, is similar to that of tBA, 2.44 Å and it reduces to 2.0 Å for $\phi_2 = 0°$, which is smaller than the sum of van der Waals radius of H, 2.1 Å. Therefore the deviation of ϕ_2 from 0° in MBBA seems to be dominated by the same interaction as in the case of tBA.

In the case of PAA, however, the two phenylene rings and the azoxy plane were practically coplanar with the dihedral angles of 11(26)° and 11(11)°.[1] The difference in ϕ_2 is explained as follows: the repulsive interaction between $H_{21}\cdots H_{29}$ is important in MBBA, while the interactions among the π electrons of the N═N bond, the N−O bond with the considerable double-bond character and the aromatic rings are more important than steric effects in PAA.

3. Comparison of Conformations in Vapor, Liquid-Crystal, and Solid Phases. To our knowledge, only one experimental investigation has been reported for MBBA in the gas phase. It is the study of the UV absorption spectrum of gaseous MBBA recorded at 110 °C.[24] In this study, ϕ_2 was estimated to be 66.5° by comparing the intensity ratio of the $\pi\pi^*$ and $n\pi^*$ bands with its simulated values by the CNDO/2 method, but no error estimation was given for the ϕ_2 value. Considering the reliability of the band intensity measurement and the CNDO/2 calculation, the discrepancy between this result and ours (66.5° vs 48(9)°) does not seem to be substantial.

In the nematic phase, the resulting ϕ_2 values of MBBA with deuterated rings were estimated as a function of temperature by deuteron magnetic resonance.[4a] The ϕ_2 angle was found to be temperature sensitive, e.g., $\phi_2 = 39°$ at 33 °C and $\phi_2 = 44°$ at 35 °C. A recent two-dimensional NMR study[4b] reported the ϕ_2 value of 33(5)° which was comparable with the values of 24° and 43° determined in the previous NMR studies.[4c,d] The comparison of the GED value with these NMR data shows that the ϕ_2 angle slightly increases on going from the nematic phase to the gas phase. This is consistent with the results reported in ref 24. As for the ϕ_1 in the nematic phase, two values, 20(10)° and 0°, have been reported in refs 4b and d, indicating that the ϕ_1 is not sensitive to the intermolecular interactions.

TABLE 6. Comparison with the Dihedral Angles of MBBA Determined by X-ray Diffraction

	gas[b]	crystal[c]		
dihedral angles[a]	TT	**I**	**II**	**III**
ϕ_1	0 (12)	4	−1	−3
ϕ_2	48 (9)	24	−29	−1
ϕ_3	0[d]	176	−1	−179
ϕ_4	88[d]	67	−96	−99
ϕ_5	180[d]	174	−177	180
ϕ_6	180[d]	−179	−69	174
ϕ_7	180[d]	−177	176	179

[a] Dihedral angles in degrees. ϕ_1, ϕ_2, ϕ_3, ϕ_4, ϕ_5, ϕ_6, and ϕ_7 denote dihedral angles $N_1C_2C_3C_8$, $C_2N_1C_9C_{14}$, $C_5C_6O_{15}C_{16}$, $C_{11}C_{12}C_{17}C_{18}$, $C_{12}C_{17}C_{18}C_{19}$, $C_{17}C_{18}C_{19}C_{20}$, and $C_9N_1C_2C_3$, respectively (see Figure 1 for atom numbering). [b] This work. [c] Calculated from the atomic coordinates of conformers at three sites reported in reference 3. [d] Assumed.

As shown in Table 4, the bond distances and angles in the crystal approximately agree with those in the gas phase. Table 6 shows the dihedral angles, $\phi_1-\phi_7$, of the three conformers of MBBA in the crystal determined by X-ray diffraction. The ϕ_2 value in the gas phase is larger than that in the crystalline state. Therefore this observation clearly shows the influence of crystal packing on the molecular conformation of MBBA. The ϕ_1 value in the gas-phase agrees with that in the crystalline state. The two values, 20(10)° and 0°, determined by NMR in the nematic phase,[4b,4d] also indicate that ϕ_1 is rather insensitive to intermolecular interactions.

Two configurations exist for the terminal butyl group in the crystal of MBBA (see ϕ_5 and ϕ_6 in Table 6). The butyl groups of molecules **I** and **III** have *trans*−*trans* configurations (TT). Molecule **II** has a gauche conformation with respect to ϕ_6 (TG). Boese et al. [3] have noted that the distances between the end carbon atoms (C_{16} and C_{20}) of these conformers are nearly the same, 15.5−15.9 Å.

Table 3 shows that the $C_{16}\cdots C_{20}$ distances of the four configurations of the butyl group determined by GED are 15.8, 15.9, 14.3, and 14.1 Å for conformers TT, TG, GT, and GG, respectively. Therefore the molecular lengths of the GT and GG conformers are shorter than the TT and TG conformers by about 1.5 Å and the TT and TG have more rodlike shapes (see Figure 1). Thus it is considered that the rodlike shape is more stabilized in the crystal of MBBA.

4. Transition Temperature and the Molecular Geometry. The transition temperature T_{N-I} from the nematic to the liquid phase of MBBA is much lower than that of PAA (47 vs 137 °C). This is consistent with the general tendency that the mesogen of the type $R-C_6H_4-CH=N-C_6H_4-R'$ has a lower T_{N-I} than the type $R-C_6H_4-N=NO-C_6H_4-R'$.[45] In ref 45, it is suggested that this difference in T_{N-I} comes from the difference in the length and the planarity of the core. Our GED studies on MBBA (−CH═N− type) and PAA (−N═NO− type) have revealed that the lengths of the core ($C_6\cdots C_{12}$) of these types are almost equal to each other (9.2 Å for MBBA and 9.1 Å for PAA[1]). On the other hand, it has been found out that MBBA has a nonplanar core and PAA has a nearly planar one in the gas phase. Therefore it can be concluded that the difference between the T_{N-I} of −CH═N− and −N═NO− types comes not from the difference in the lengths of the core but from that in the core planarity. Of course, in the comparison between MBBA and PAA, the flexible tail of the former (*n*-butyl group) is considered to have additional contribution to decreasing its T_{N-I} and the effect of anisotropy of polarizability cannot be ruled out.

Acknowledgment. We thank the Ministry of Education, Science and Culture for grants in aid for scientific research (Grants 08454168 and 03740256). G. F. thanks the Research Fund of Hungary, OTKA, Grant T017374, for financial support. We thank the Computer Center, Institute for Molecular Science, Okazaki National Research Institutes, for the use of the Hitac Model S-820/80, Hitac Model H-682H, and NEC SX-3/34R computers and GAUSSIAN 86 and GAUSSIAN 92 programs (IMS versions). Data analysis was performed using the Hitac Models M-880 and S-820/80 at the Hokkaido University Computing Center.

Supporting Information Available: Tables and figures of the leveled total intensities and the backgrounds, optimized geometrical parameters of the four conformers, the local symmetry coordinates, the valence force constants, the observed and calculated frequencies with potential energy distributions, the structural parameters, and the HF/4-21G(*) constraints adopted in the data analysis of GED, and the correlation matrix. Supporting Information is available free of charge via the Internet at http://pubs.acs.org.

References and Notes

(1) Kuze, N.; Ebizuka, M.; Fujiwara, H.; Takeuchi, H.; Egawa, T.; Konaka, S.; Fogarasi, G. *J. Phys. Chem.* A **1998**, *102*, 2080.

(2) Sereda, S. V.; Timofeeva, T. V.; Antipin, M. Y.; Struchkov, Y. T. *Liq. Cryst.* **1992**, *11*, 839.

(3) Boese, R.; Antipin, M. Y.; Nussbaumer, M.; Bläser, D. *Liq. Cryst.* **1992**, *12*, 431.

(4) (a) Dong, R. Y.; Tomchuk, E.; Wade, C. G.; Visintainer, J. J.; Bock, E. *J. Chem. Phys.* **1977**, *66*, 4121. (b) Hoshino, T.; Kubo, A.; Imashiro, F.; Terao, T. *Mol. Phys.* **1998**, *93*, 301. (c) Prasad, J. S. *J. Chem. Phys.* **1976**, *65*, 941. (d) Höhener, A.; Müller, L.; Ernst, R. R. *Mol. Phys.* **1979**, *38*, 909.

(5) Minkin, V. I.; Zhdanov, Y. A.; Medyantzeva, E. A.; Ostroumov, Y. A. *Tetrahedron* **1967**, *23*, 3651.

(6) Akaba, R.; Tokumaru, K.; Kobayashi, T. *Bull. Chem. Soc. Jpn.* **1980**, *53*, 1993.

(7) Akaba, R.; Sakuragi, H.; Tokumaru, K. *Bull. Chem. Soc. Jpn.* **1985**, *58*, 1186.

(8) Pivovarova, N. S.; Boldeskul, I. E.; Shelyagenko, S. V.; Fialkov, Y. A. *J. Mol. Struct.* **1988**, *174*, 297.

(9) Schäfer, L.; Ewbank, J. D.; Siam, K.; Chiu, N.; Sellers, H. L. *Stereochemical Applications of Gas-Phase Electron Diffraction Part A—The Electron Diffraction Technique*; Hargittai, I., Hargittai, M., Eds.; VCH Publishers: New York, 1988; Chapter 9.

(10) Konaka, S.; Kimura, M. In *13th Austin Symposium on Gas-Phase Molecular Structure, 12−14 March 1990*; The University of Texas, Austin, TX, 1990; S21.

(11) Tsuboyama, A.; Murayama, A.; Konaka, S.; Kimura, M. *J. Mol. Struct.* **1984**, *118*, 351.

(12) Kimura, M.; Konaka, S.; Ogasawara, M. *J. Chem. Phys.* **1967**, *46*, 2599.

(13) Tavard, C.; Nicolas, D.; Rouault, M. *J. Chim. Phys. Phys.-Chim. Biol.* **1967**, *64*, 540.

(14) Pulay, P.; Fogarasi, G.; Pang, F.; Boggs, J. E. *J. Am. Chem. Soc.* **1979**, *101*, 2550.

(15) Frisch, M. J.; Binkley, J. S.; Schlegel, H. B.; Raghavachari, K.; Melius, C. F.; Martin, R. L.; Stewart, J. J. P.; Bobrowicz, F. W.; Rohlfing, C. M.; Kahn, L. R.; DeFrees, D. J.; Seeger, R.; Whiteside, R. A.; Fox, D. J.; Fluder, E. M.; Topiol, S.; Pople, J. A. *GAUSSIAN 86*; Carnegie-Mellon Quantum Chemistry Publishing Unit, Carnegie-Mellon University: Pittsburgh, PA, 1984.

(16) Frisch, M. J.; Trucks, G. W.; Head-Gordon, M.; Gill, P. M. W.; Wong, M. W.; Foresman, J. B.; Johnson, B. G.; Schlegel, H. B.; Robb, M. A.; Replogle, E. S.; Gomperts, R.; Andres, J. L.; Raghavachari, K.; Binkley, J. S.; Gonzalez, C.; Martin, R. L.; Fox, D. J.; DeFrees, D. J.; Baker, J.; Stewart, J. J. P.; Pople, J. A. *GAUSSIAN 92*, Revision F.3; Gaussian, Inc.: Pittsburgh, PA, 1992.

(17) Pulay, P. *TX90 Program Description*; University of Arkansas: Fayetteville, AR, 1990.

(18) Fogarasi, G.; Zhou, X.; Taylor, P. W.; Pulay, P. *J. Am. Chem. Soc.* **1992**, *114*, 8191.

(19) Vergoten, G.; Fleury, G. *Mol. Cryst. Liq. Cryst.* **1975**, *30*, 213.

(20) Vergoten, G.; Fleury, G.; Jones, R. N.; Nadeau, A. *Mol. Cryst. Liq. Cryst.* **1976**, *36*, 327.

(21) Derollez, P.; Bee, M.; Jobic, H. *Spectrochim. Acta* **1992**, *48*, 743.

(22) Destrade, C.; Gasparoux, H. *J. Phys. Lett.* **1975**, *36*, 105.

(23) Sciesinska, E.; Sciesinski, J.; Twardowski, J.; Janik, J. A. *Mol. Cryst. Liq. Cryst.* **1974**, *27*, 125.

(24) Mizuno, M.; Shinoda, T. *Mol. Cryst. Liq. Cryst.* **1981**, *69*, 103.

(25) Vergoten, G.; Fleury, G. *J. Mol. Struct.* **1976**, *30*, 347.

(26) Figueroa, K.; Campos-Vallette, M.; Rey-Lafon, M. *Spectrochim. Acta* **1990**, *46A*, 1659.

(27) Kozhevina, L. I.; Prokopenko, E. B.; Rybachenko, V. I.; Titov, E. V. *J. Mol. Struct.* **1993**, *295*, 53.

(28) Meimć, Z.; Baranovi, M, G. *Pure and Appl. Chem.* **1989**, *61*, 2129.

(29) Meić, Z.; Baranović, M, G.; Šuste, T. *J. Mol. Struct.* **1993**, *296*, 163.

(30) Balfour, W. J. *Spectrochim. Acta* **1983**, *39A*, 795.

(31) Owen, N. L.; Hester, R. E. *Spectrochim. Acta* **1969**, *25A*, 343.

(32) Lau, C. L.; Snyder, R. G. *Spectrochim. Acta* **1971**, *27A*, 2073.

(33) Boerio, F. J.; Bahl, S. K. *Spectrochim. Acta* **1976**, *32A*, 987.

(34) Varsányi, G. *Assignments for Vibrational Spectra of Seven Hundred Benzene Derivatives*; Akadémial Kiadó; Budapest, and Adam Hilger Ltd: London: 1974.

(35) Snyder, R. G.; Schachtschneider, J. H. *Spectrochim. Acta* **1965**, *21*, 169.

(36) Harada, I.; Takeuchi, H.; Sakakibara, M.; Matsuura, H.; Shimanouchi, T. *Bull. Chem. Soc. Jpn.* **1977**, *50*, 102.

(37) Snyder, R. G.; Zerbi, G. *Spectrochim. Acta* **1967**, *23*, 391.

(38) Brunvoll, J.; Bohn, R. K.; Hargittai, I. *J. Mol. Struct.* **1985**, *129*, 81.

(39) Kuchitsu, K.; Cyvin, S. J. *Molecular Structures and Vibrations*; Cyvin, S. J., Ed.; Elsevier: Amsterdam, 1972; Chapter 12.

(40) Kuze, N.; Takeuchi, H.; Egawa, T.; Konaka, S.; Newton, S. Q.; Schäfer, L. *J. Mol. Struct.* **1993**, *291*, 11.

(41) Traetteberg, M.; Hilmo, I.; Abraham, R. J.; Ljunggren, S. *J. Mol. Struct.* **1978**, *48*, 395.

(42) Naumov, V. A.; Litvinov, O. A.; Kibardin, A. M. *Zh. Strukt. Khim.* **1984**, *25*, 35.

(43) Vilkov, L. V.; Sadova, N. I. *Stereochemical Applications of Gas-Phase Electron Diffraction Part B—Structural Information for Selected Classes of Compounds*; Hargittai, I., Hargittai, M., Eds.; VCH Publishers: New York, 1988; Chapter 2.

(44) Seip, H. M.; Seip, R. *Acta Chem. Scand.* **1973**, *27*, 4024.

(45) Gray, G. W. *The Molecular Physics of Liquid Crystals*; Luckhurst, G. R.; Gray, G. W., Ed.; Academic Press: London, 1979: Chapter 1.